

Submitted to *The Astrophysical Journal*

Far Ultraviolet Spectra of B Stars near the Ecliptic¹

Carmen Morales, Verónica Orozco, José F. Gómez

Laboratorio de Astrofísica Espacial y Física Fundamental, INTA, Apdo. Correos 50727,
E-28080 Madrid, Spain

Joaquín Trapero

Universidad SEK, Cardenal Zúñiga s/n, E-40003 Segovia, Spain, and Laboratorio de
Astrofísica Espacial y Física Fundamental, INTA

Antonio Talavera

Laboratorio de Astrofísica Espacial y Física Fundamental, INTA

Stuart Bowyer, Jerry Edelstein, Eric Korpela, Michael Lampton

Space Sciences Laboratory, University of California, Berkeley, CA 94720–7304

Jeremy J. Drake

Harvard-Smithsonian Center for Astrophysics, MS-3, 60 Garden Street, Cambridge, MA
02138

ABSTRACT

Spectra of B stars in the wavelength range of 911–1100 Å have been obtained with the EURD spectrograph onboard the Spanish satellite MINISAT-01 with ~ 5 Å spectral resolution. IUE spectra of the same stars have been used to normalize Kurucz models to the distance, reddening and spectral type of the corresponding star. The comparison of 8 main-sequence stars studied in detail (α Vir, ϵ Tau, λ Tau, τ Tau, α Leo, ζ Lib, θ Oph, and σ Sgr) shows agreement with Kurucz models, but observed fluxes are 10–40% higher than the models in most cases. The difference in flux between observations and models is higher in the wavelength range between Lyman α and Lyman β . We suggest that Kurucz models underestimate the FUV flux of main-sequence B stars between these

¹Based on the development and utilization of the Espectrógrafo Ultravioleta de Radiación Difusa, a collaboration of the Spanish Instituto Nacional de Técnica Aeroespacial and the Center for EUV Astrophysics, University of California, Berkeley

two Lyman lines. Computation of flux distributions of line-blanketed model atmospheres including non-LTE effects suggests that this flux underestimate could be due to departures from LTE, although other causes cannot be ruled out. We found the common assumption of solar metallicity for young disk stars should be made with care, since small deviations can have a significant impact on FUV model fluxes. Two peculiar stars (ρ Leo and ϵ Aqr), and two emission line stars (ϵ Cap and π Aqr) were also studied. Of these, only ϵ Aqr has a flux in agreement with the models. The rest have strong variability in the IUE range and/or uncertain reddening, which makes the comparison with models difficult.

Subject headings: Stars: atmospheres — stars: early-type — ultraviolet: stars

1. Introduction

The far ultraviolet (FUV) spectral region is one of the least studied ranges in stellar physics. IUE and HST have provided a large number of stellar spectra at wavelengths longer than 1100 Å. However, data at wavelengths below 1100 Å are much more limited. Observations by Voyager (Broadfoot et al. 1977), Copernicus (Rogerson et al. 1973), HUT (Davidsen 1990), ORFEUS (Hurwitz & Bowyer 1991), and UVSTAR (Stalio et al. 1993), and rocket observations by Brune, Mount, & Feldman (1979), Carruthers, Heckathorn, & Opal (1981), have provided some data. The absolute fluxes obtained by these investigations are often highly discrepant for a variety of reasons.

In a previous work (Morales et al. 2000), we reported on FUV spectroscopic observations of the bright star α Vir (Spica) obtained with the EURD spectrograph, which provided an absolute flux for this star. EURD data on α Vir were reasonably well reproduced by Kurucz models (Kurucz 1993) fitted to IUE data.

In this paper, we present spectra of stars observed by EURD during its first two years of operation. Although the design of this spectrograph is optimized to study diffuse radiation, it can detect bright, early-type stars in the FUV. In §2 we present the observations, data reduction, and our use of IUE data. In §3 we present our results for main sequence stars and compare them with model atmospheres. In §4 we discuss the peculiar and emission line stars observed. We summarize our conclusions in §5.

2. Observations, Data Reduction and Merged IUE Spectra

EURD is one of the instruments onboard the Spanish satellite MINISAT-01. It consists of two spectrographs covering the bandpass between 350 and 1100 Å, with ~ 5 Å spectral resolution. MINISAT-01 was launched on April 21, 1997. Its orbit is retrograde with an inclination of 151° and an altitude of 517 km. The design of the spectrographs and their ground calibrations are described in detail in Bowyer, Edelstein, & Lampton (1997).

EURD samples the entire ecliptic plane once per year using nightly observations in the anti-sun direction. The EURD spectrographs perform simultaneous observations with a field of view of $25^\circ \times 8^\circ$. Stars with ecliptic latitudes between -13° and $+13^\circ$ can, in principle, be detected by EURD. However, only those between -4° and $+4^\circ$ are certain to fall into the field of view. The 12 stars presented in this paper are those which have been observed up to March 31, 1999. Other stars were detected in these EURD data, however obtaining their spectra was impossible because of spectral confusion from other stars simultaneously in the field of view. EURD has detected stellar emission only from 912 to 1100 Å due to the absorption by the interstellar medium.

The data reduction process consists of identifying and separating stellar point-source emission from the instrumental noise and diffuse emission produced by strong geocoronal airglow emission lines and possibly by the hot component of the interstellar medium. The photon counting detector records images with spectral resolution (~ 5 Å) in one axis and angular resolution ($\sim 10'$) in the other axis. When a star falls in the field of view of the instrument, its spectra is distributed within a finite area in the angular dimension. In contrast, instrumental background and diffuse emission will be located along the entire angular dimension. To test for the presence of a stellar source, we accumulated an entire detector image every 28 seconds. The detector image was integrated over the spectral dimension to obtain a histogram of total spectral intensity as a function of field-view angle. If the maximum of the histogram exceeded 4 times the noise level, defined as the standard deviation of the continuum level of the histogram, then a stellar spectrum was obtained from the flux found within 7 angular pixels ($10'.5$) of the maximum. A net stellar spectrum was derived by subtracting the atmospheric and instrumental background taken from an equivalent area adjacent to the stellar region. The net spectrum's intensity was corrected using the inflight-calibrated variation of optical efficiency as a function of radiation input angle (determined with observations of α Vir during April 1999). Intensity-corrected spectra were co-added for each stellar object and converted to fluxes, applying the in-flight calibration performed using simultaneous observations of the full Moon with EUVE and EURD. Further details of the data reduction process can be found in Gómez et al. (2000).

We have obtained spectra of 12 B stars taken over two years of observations. Table 1

shows the dates of the observations. The total integration times and statistical significance are shown in Table 2. Fig. 1 shows the spectra for all the stars except HD 116658 (α Vir), which has been previously published in Morales et al. (2000).

We have divided the stars into three groups: main-sequence, peculiar, and emission line stars. The parameters of the stars in these groups are shown in Table 3. Spectral types and V magnitudes are from the Simbad database, color excesses are obtained using the intrinsic (Warren 1976) and observed (b-y) color (Hauck & Mermilliod 1998), and the relation of Penprase (1992) between E(b-y) and E(B-V). Effective temperatures are deduced from the comparison of Kurucz models (see §3) only for main-sequence stars, due to the uncertainties found in model fitting for peculiar and emission line stars (see §4 below).

IUE spectra of the observed stars were selected from the INES database, according to their quality. Only large aperture, not trailed observations were taken. In the case of HD 157056 the only available short wavelength IUE spectrum is of small aperture and has been normalized to fit the large aperture long wavelength spectrum of this star. Spectra from SWP and LWP cameras were joined at 1940 Å, truncating SWP spectra longward of 1940 Å and LWP spectra shortward of 1940 Å. IUE spectra used in this paper are shown in Table 4. The IUE absolute flux calibration defined for the final archive used in this work is 7.2 – 10 % lower than the Hubble Space Telescope flux scale (González-Riestra 1998, Massa & Fitzpatrick 2000).

3. Main Sequence Spectra and Comparisons with Model Atmospheres

We have compared our data with the Kurucz (1993) atmosphere models, extracted from the homogeneous grid of models of Lejeune, Cuisinier, & Buser (1997). The comparison with Kurucz models is done with the same method we used for α Vir, binning IUE and EURD spectra to the 10 Å spectral resolution of the models and dereddening them with the Cardelli, Clayton, & Mathis (1989) extinction law. Between 912 and 1100 Å this law was extrapolated by polynomial fit, as suggested by Longo et al. (1989). However instead of fixing the temperature, which is not well known for the stars of the present sample, we took the temperature of the model that best fits the IUE range longward of 1246 Å (in order to avoid the Lyman α geocoronal component present in IUE spectra), using the IDL program KSCALE of the IUE RDAF Library, that searches for the minimum rms deviation between models and data. Thus, the temperatures derived by this fit do not depend on absolute flux, only on the shape of the spectra. The values of the stellar radii deduced from the fit to IUE (assuming Hipparcos distances, ESA 1997) are within the values, obtained by different methods, reported by Fracassini et al. (1988).

Atmosphere models of solar composition, microturbulent velocity $v_t = 2.0$, and gravity $\log g = 4.0$ were taken for main-sequence stars. A ratio of total to selective extinction $R = 3.1$ was used for all the stars except for HD 138485 which is located in the Upper Scorpius association. Gutiérrez-Moreno & Moreno (1968) found for this part of the association a value of $R = 6$. Using Hipparcos distances (ESA 1997) and more recent spectral types from the Simbad database for 44 stars belonging to the Upper Scorpius association, we also found $R=6$ for this region. This value was used to deredden HD 138485.

In Fig. 2 we show the reddened Kurucz model that best fits the IUE range, and the whole IUE and EURD spectra for HD 23793. Fig. 3 shows the comparison of EURD and IUE data with models for all main-sequence stars. EURD spectra and the appropriate Kurucz models show a general agreement, with the best agreement occurring at wavelengths shorter than Lyman β (1026 Å). EURD integrated fluxes shortward of 1010 Å are 10 to 40% higher than Kurucz fluxes in most cases (see Table 3), while for wavelengths longward of Lyman β , the EURD flux can exceed the model values by up to 95% for the worst case (HD 87901 [α Leo], see Fig. 3). This confirms the result obtained for EURD observations of α Vir (Morales et al. 2000) that also found higher fluxes than expected from the models. If we correct the IUE absolute flux calibration to match the HST flux calibration, the agreement with the models improves except for the stars with negative difference (HD 25204 and HD 175191). Only HD 138485 shows slightly less flux than the models longward of Lyman β , but this could reflect the uncertainty in the value of $R=6$ used for dereddening.

The same trend of observed fluxes higher than the models can be seen in IUE spectra shortward of Lyman α (1216 Å) for HD 23793, HD 25204 and HD 29763, and HD 87901, although high fluxes at longest EURD wavelengths and shortest IUE ones could be due to edge effects in the detectors. In fact, errors have been found to be systematically higher at IUE shortest wavelengths (Massa & Fitzpatrick 2000). However, Voyager data, which have the region between Lyman α and Lyman β in the middle of their detectors, agree with EURD fluxes for the two stars they have in common, α Vir and α Leo. Fig. 4 shows a comparison of EURD and Voyager observations with the corresponding model for α Leo, which shows the highest discrepancy from models at the longest EURD wavelengths. It is obvious that both observations closely agree with each other, and are significantly higher than the model. The agreement between Voyager and EURD is also remarkable for α Vir (Morales et al. 2000), both being higher than the corresponding atmosphere model.

Main-sequence B stars are thought to be relatively well understood in terms of the modeling of their photospheres. However, as discussed earlier, there have been relatively few studies in the FUV to test available models. The discrepancies we found between observed and model fluxes could in principle arise from several different sources: EURD

instrument calibration errors; inappropriate ISM reddening corrections; deficiencies in the Kurucz LTE model atmosphere; or errors in the adopted model stellar parameters.

An incorrect EURD calibration might be responsible for the discrepancy. However, the detailed character of our inflight calibration and the agreement in observed fluxes for two stars, α Vir and α Leo, observed by both *Voyager* and EURD, using independent calibrations (with white dwarfs and the Moon respectively), give support to the correctness of our calibration.

Significant problems associated with our extinction corrections also seem unlikely. While accurate corrections for the effects of ISM absorption and scattering in the FUV is a difficult problem (e.g., Savage et al. 1985), all of our stars have very low values of reddening and consequently any uncertainty will be small. Though early results from a survey of interstellar H_2 made by FUSE have indicated an ubiquitous presence of H_2 (Tumlinson et al. 1999), we have not applied corrections for H_2 absorption because the H_2 columns toward these targets are small and the effects should be negligible. We have verified this assumption by computing the H_2 absorption in the 900-1100 Å range seen at the resolution of the EURD instrument. The relatively narrow molecular bands begin to saturate at quite low H_2 columns ($< 10^{18} \text{ cm}^{-2}$). However, they account for relatively little net flux loss at these columns when integrated over the EURD response function. This same result was found by Snow, Allen & Polidan (1990) for the case of *Voyager* spectra: for a H_2 column of 10^{18} cm^{-2} (a value higher than that expected for any of the main-sequence stars in our sample) the net absorption amounts to less than 5 %. We do note that a value of $R=1.0$ would increase model FUV fluxes without distorting the IUE range very much, but this value of R is very unlikely (He et al. 1995)

We suggest that Kurucz atmosphere models underestimate fluxes between Lyman α and Lyman β . It is worth noting that other authors studying stellar spectra in this wavelength range have also found discrepancies in the same direction between their observations and Kurucz models (e.g., Chavez, Stalio, & Holberg 1995; Buss, Kruk, & Ferguson 1995; Dixon & Hurwitz 1998).

An important assumption used in the Kurucz model atmospheres adopted in this study is that of LTE. In order to investigate the effects of relaxing this assumption, we have carried out new calculations using the TLUSTY model atmosphere program (Hubeny & Lanz 1995; Hubeny 2000, private communication) that uses extensive line-blanketing and that treats H, He and abundant metals fully in non-LTE in both line and continuum processes. TLUSTY model atmospheres for representative effective temperatures of 15000 K and 20000 K, with a surface gravity of $\log g = 4.0$ and solar metallicity ($[M/H]= 0.0$), were computed both under the assumption of LTE and also with the LTE assumption relaxed. In addition, a

slightly cooler model with effective temperature of 13500 K was added because of the rapid change in this temperature regime in important continuum opacity sources from neutral C, N and O to once ionized species in the FUV region.

In terms of temperature structure, the LTE and non-LTE models are very similar in the deepest layers at all the effective temperatures investigated, as expected. Toward higher layers in the line-forming regions, the LTE models are slightly hotter than the non-LTE models by up to 400 K or so. In the outer layers this situation is reversed, with the non-LTE models ending up hotter but by a larger amount of about 1500 K. We have computed the resulting synthetic spectra using the LTE and non-LTE models; comparisons for the 15000 K models are illustrated in Figure 5, binned at a resolution commensurate to that of the IUE spectra used to determine the stellar effective temperatures. We also illustrate the corresponding Kurucz model as a grey shaded region.

For the IUE spectral range, although the forms of the LTE and non-LTE model spectra appear quite similar, many differences in the various more prominent absorption lines become readily apparent when examining these model spectra at high spectral resolution. At the lower resolution of the observations however, these differences become washed out and the emergent fluxes in each spectral bin are in general similar. The situation changes in the FUV range of interest for our EURD observations: it is immediately apparent that the non-LTE model fluxes are substantially higher overall than the LTE fluxes, especially in the region between Lyman α and β . For the FUV spectral range between Lyman α and β , differences between non-LTE and LTE model fluxes increase from longer to shorter wavelengths, amounting to as much as 30 % or so near 1050 Å. Toward wavelengths shortward of Lyman β , LTE and non-LTE model fluxes converge slightly and are in somewhat better agreement.

Comparisons between hotter and cooler temperature models reveal an interesting trend. In the case of the hotter 20000 K model, the differences between LTE and non-LTE fluxes are in the same sense as for the 15000 K model, but they are significantly smaller and amount to only 10 % or so near 1050 Å. Agreement throughout the IUE range is also slightly better. In contrast, comparison of the slightly cooler 13500 K models reveals *even larger differences* between LTE and non-LTE fluxes than for the 15000 K models, amounting to approximately a factor of 2 at 1050 Å. In all cases the differences are reduced again toward wavelengths shortward of Lyman β . We note that the trend of increasing disparity between LTE and non-LTE model fluxes with decreasing effective temperature, especially near 1050 Å, is similar to the discrepancies between observations and LTE models, which are most pronounced for the coolest star of the sample.

We also note that the wavelength regime in which the non-LTE effects appear most

significant supports our method of deriving effective temperatures based on IUE fluxes longward of Lyman α , where non-LTE effects appear comparatively small at IUE resolution. At the same time, our findings suggest difficulties for methods hoping to use FUV fluxes for the derivation of effective temperatures based on synthetic LTE spectral indices.

Making the straightforward conclusion that non-LTE effects must be responsible for the model and observed FUV flux disparities in our program main-sequence B stars is complicated by the comparison between the TLUSTY LTE and Kurucz LTE models. It is apparent from Figure 5 that these are also not in good agreement in the FUV range. The Kurucz model predicts more FUV flux than the TLUSTY model. The reason for these discrepancies is not obvious, though it may be related to differences in the line and continuum opacities employed. Taking just the LTE models, the Kurucz models are in better agreement with the observations than the TLUSTY LTE models. However the *differential* comparison of TLUSTY LTE and non-LTE models is valid and these non-LTE effects will be in operation in late B star photospheres. Therefore, while the problem as to the best model formulation for the FUV range must remain unanswered, we conclude that at least some, and perhaps all, of the differences we are observing between model and EURD fluxes are caused by departures from LTE in the photosphere.

The particular departures from LTE that give rise to the effects described above are in the continua of low Z metals that dominate the continuous opacity in the FUV region in late B stars. Neutral species such as C I are overionized in the photospheric layers, and so the opacity is reduced leading to higher fluxes in the regions affected. Toward higher effective temperatures the neutrals become more minor species and cease to dominate the continuous opacity; departures from LTE in these species are therefore less important.

We have also investigated the sensitivity of the Kurucz model FUV fluxes to the stellar parameters: effective temperature, surface gravity and metallicity. There are surprisingly few modern, detailed, high resolution spectroscopic studies available for main-sequence B field stars on which to draw for guidance as to the exact parameters and compositions of our target stars. As has been discussed by previous authors, the effective temperature scale of B main-sequence stars is dependent to a significant extent on the indices used to derive it, even down to different UV indices (e.g. Chavez et al. 1995; Buss et al. 1995). Moreover, it is well known that the FUV fluxes of B main-sequence stars are very sensitive to the effective temperature adopted. Indeed, the 500-1000 K higher effective temperatures derived by Buss et al. (1995) based on *HUT* FUV fluxes are a direct result of the same excess observed flux at short wavelengths as is evident in our EURD spectra. What is less often discussed is the effects of surface gravity and metallicity on these fluxes (see Fitzpatrick & Massa 1999, for a discussion on their effects on UV-optical fluxes).

We illustrate the FUV flux sensitivity to model parameters for the case of the $T_{eff} = 15000$ K model in Figure 6. As expected, strong sensitivity to temperature is shown by the comparison with a model 2000 K cooler, but with otherwise similar parameters. The flux disparity increases toward shorter wavelengths as expected from the analogous black body behavior. A difference of 2000 K in effective temperature is much larger than any uncertainties in the derivation of temperature scales, but it is clear that even adopting model parameters a few hundred degrees different would significantly alter the predicted fluxes in the very shortest wavelengths. The flux discrepancy we are seeing for α Leo is not simply an error in the adopted effective temperature. This is clear in view of the nature of the discrepancy: instead of increasing with decreasing wavelength, the model and observations are actually in much better agreement below 1000 Å than above.

It is also clear from Figure 6 that stellar FUV fluxes are not strongly dependent on the exact value of surface gravity adopted. Reducing the surface gravity leads to a *decrease* in the FUV flux and a slight *increase* in the flux at the longest UV wavelengths. Thus, for the case of a typical B star in our study, an error in the adopted surface gravity is likely to be at least partially compensated for by the derivation of a slightly different effective temperature. The resulting predicted FUV fluxes *seen at the resolution of our instrument* would be corrected for by a compensatory temperature error.

The value adopted for the metallicity is much more important. Previous FUV studies appear to have assumed that the metallicities of all early-type stars are identically equal to the solar value (Chavez et al. 1995; Buss et al. 1995). Studies of disk stars and young stars formed in very similar ISM environments show this not to be the case at levels that could be significant for FUV fluxes. The studies of abundances in main-sequence B stars in the Orion association by Cunha & Lambert (1992, 1994) revealed differences in O and Si abundances of as much as 0.2 dex in stars co-located on the sky and at similar distances. They conjectured that these differences arose because they were formed from different regions of a parent molecular cloud enriched to different extents with the ejecta of Type II supernovae. On a much wider scale, young stars in the solar neighborhood also exhibit significant scatter in metallicity amounting to ± 0.2 dex or so about the solar value (e.g. Luck & Lambert 1985; Nissen 1988; Boesgaard 1989; Edvardsson et al. 1993). Assumption of solar metallicity for young disk stars should therefore only be done under peril of errors of up to 50 %.

By inspection of Figure 6, we note a difference in FUV flux shortward of Lyman β of as much as 30 % for a model differing in metallicity by 0.5 dex, with the change occurring in the obvious sense that lower metallicity, leading to lower FUV opacity, leads to higher FUV fluxes. Consequently, care should be taken in the adoption of the metallicity parameter if

comparison is to be meaningful at a level of order 15 % or better.

Another possible stellar parameter that can have an important effect on FUV fluxes is microturbulent velocity. Fitzpatrick & Massa (1999) have found a dependence of UV flux on this parameter that is of the same order as the effect of surface gravity and metallicity. However, their calculation does not extend to the FUV. Therefore it would be interesting to investigate the impact of microturbulent velocity in the EURD range.

In the particular case of α Leo, we note that its rotational velocity ($v = 350 \text{ km s}^{-1}$, Bernacca & Perinotto 1970) could also be important to interpret its large FUV flux excess. Model calculations by Collins & Sonneborn (1977) predict a flux dependency on rotational velocity that becomes more significant in the FUV, for B0-F8 stars. However this effect has not been found observationally (Molnar, Stephens & Mallama 1978, Llorente de Andrés & Morales 1979). On the other hand, it has been suggested that rotational velocities may induce an effective color excess for spectral types earlier than B6 (Maeder 1975, Llorente de Andrés et al. 1981), which if neglected, would result in a spurious ultraviolet excess. This would not be the case for α Leo, a B7 star, and we suggest that its high rotational velocity do not have a significant impact on its FUV flux excess.

4. Peculiar Stars and Emission Line Stars

We obtained spectra of two peculiar stars. However, the strong influence of metallicity in the far ultraviolet fluxes of model atmospheres makes comparisons with models difficult for these stars. An accurate knowledge of this stellar parameter is necessary in order to find the appropriate model to compare with the observations. The two peculiar stars we observed were:

HD 210424. A suspected chemically peculiar star of the Si type in the catalog of Renson, Gerbaldi, & Catalano (1991). Cayrel de Strobel et al. (1997) found a metal abundance of $[\text{Fe}/\text{H}] = -0.26$, while Leone, Manfré, & Catalano (1995), with optical high resolution spectroscopy, could not find any sign of metallicity, while the overall flux distribution could be reproduced using a Kurucz model (ATLAS9) with solar abundance. This, together with flux differences of 20% among IUE observations at $\lambda > 1400 \text{ \AA}$ makes the comparison with model atmospheres difficult. With both values of metallicity EURD fluxes are two to three times higher than any possible model fitted to the IUE wavelength range.

HD 91316. An OBN supergiant with moderated nitrogen enhanced (Walborn 1976), with a metal abundance of $[\text{Fe}/\text{H}] = -0.89$ (Cayrel de Strobel et al. 1997). After interstellar

reddening correction of $E(B-V) = 0.056$, the EURD fluxes are well fit by a Kurucz model of 19400 K, $\log g=3.0$ and with a metallicity of -0.89 .

We obtained spectra of two emission line stars. In the study of these stars, the difficulty in evaluating the amount of emission from the central star and from the circumstellar envelope makes the determination of the interstellar extinction very complicated. Both stars in our sample show strong variability in the IUE observations. Since these observations were not simultaneous with our EURD observations, any comparisons are problematical. The two emission line stars observed were:

HD 205637. An emission line star, also classified as peculiar of the Si type by Renson et al. (1991). Neither its metal abundance, nor its real color excess (it has significant circumstellar envelope emission) are known. A well-known shell star, MWC 373 (Merrill & Burwell 1933), it is a very close system with components of magnitudes 4.9 and 6.2 at less than $0''.01$ plus another component of 9.5 at $68''$ (Catalano & Renson 1998). It is a variable star with a period of 0.9775 days (Pedersen 1979). IUE observations show a flux variability of a factor of two.

HD 212571. Classified as a shell star, MWC 388 (Merrill & Burwell 1933), IUE observations from 1979 to 1995 show a variability of $\sim 38\%$ for the whole short-wavelength IUE range. Assuming that its energy distribution is unaffected by envelope radiation in the 3700-5500 Å spectral region, Kaiser (1989) deduced an $E(B-V) = 0.11$ for the central star. Kurucz models fitted to maximum and minimum IUE data show a difference of 600 K between them, and the extension of none of them fit well the EURD range. EURD fluxes are higher than the two models fitted and also brighter than Voyager and HUT (Buss et al. 1994) observations of this star.

5. Conclusions

We have obtained the far ultraviolet spectra (shortward of 1100 Å) of 12 B-type stars, using the EURD spectrograph on-board MINISAT-01. We have carried out a detailed comparison of these spectra with several model atmosphere codes. We find:

1. Comparison with Kurucz models show that EURD fluxes for main-sequence B stars are 10-40 % higher than the model predictions in most cases for wavelengths shorter than Lyman β . This difference would be reduced using the HST calibration to correct IUE fluxes.
2. For wavelengths longer than Lyman β EURD spectra tend to show a stronger flux

excess compared with Kurucz model atmospheres for both IUE and HST absolute flux scales. A flux excess between Lyman α and β is also seen in IUE spectra for half of our main-sequence stars.

3. Comparisons between flux distributions of line-blanketed model atmospheres indicate that the non-LTE case is overionized relative to the LTE case. Non-LTE effects on low Z metals, which are important continuum opacity sources, can lead to elevated fluxes shortward of the C I edge. We therefore suggest that the observed flux excesses compared to Kurucz LTE models between Lyman α and β could be due to departures from LTE. The non-LTE effects increase with decreasing effective temperature as the neutral absorbers, though significantly overionized, become major species. At higher effective temperatures these absorbers are completely ionized and do not contribute to the opacity.
4. The common assumption of solar metallicity for young disk stars should be questioned when attempting to model the FUV flux of mid- and late-type B stars. Even fairly small deviations from the solar mixture of 0.1-0.2 dex (values typical of the scatter expected in present-day star-forming regions and in young stars in the solar neighborhood) can have a significant and observable impact on FUV fluxes that are heavily moderated by metal line blanketing.
5. For peculiar and emission line stars a precise determination of variability and metallicity is necessary to perform good comparisons between models and observations. In our data of these stars only HD 91316 could be successfully fit.

We are grateful to Jay Holberg for sending us the Voyager data. This research has made use of the SIMBAD database, operated at CDS, Strasbourg, France, and of the International Ultraviolet Explorer data retrieved from the INES Archive. The development of EURD has been partially supported by INTA grant IGE490056. V.O. and J.T. acknowledge support by Junta de Castilla y León, grant SEK1/00B. JFG is supported in part by DGESIC grant PB980670-C02 and by Junta de Andalucía (Spain).

Partial support for the development of the EURD instrument was provided by NASA grant NGR05-003-450. When NASA funds were withdrawn by Ed Weiler, the instrument was completed with funds provided by S. Bowyer. The UCB analysis and interpretation in this work was carried out through the volunteer efforts of the authors. JJD would like to extend warm thanks to Ivan Hubeny for help with computation of the non-LTE TLUSTY model atmospheres. JJD was supported by the Chandra X-ray Center NASA contract NAS8-39073 during the course of this research.

REFERENCES

- Bernacca, P.L. & Perinotto, M. 1979, *Contr. Oss. Astrof. Padova in Asiago*, 239,1
- Boesgaard, A. M. 1989, *ApJ*, 336, 798
- Bowyer, S. Edelstein J., & Lampton, M. 1997, *ApJ*, 485, 523
- Broadfoot, A. L., Sandel, B. R., Shemansky, D. E., Atreya, S. K., Donahue, T. M., Moos, H. W., Bertaux, J. L., Blamont, J. E., Ajello, J. M., Strobel, D. F., McConnell, J.C., Dalgarno, A., Goody, R., McElroy, M. B., & Yung, Y. L. 1977, *Space Sci. Rev.* 21,183
- Brune, W. H., Mount, G. H., & Feldman, P. D. 1979, *ApJ*, 227, 884
- Buss, R. H., Allen, M., McCandliss, S., Kruk, J. W., Liu, J.-Ch. & Brown, T. 1994, *ApJ*, 430, 630
- Buss, R. H., Kruk, J. W., & Ferguson, H. C. 1995, *ApJ*, 454, L55
- Cardelli, J. A., Clayton, G. C., & Mathis J. S. 1989, *ApJ*, 345, 245
- Carruthers, G. R., Heckathorn, H. M., & Opal, C. B. 1981, *ApJ*, 243, 855
- Catalano, F. A., & Renson, P. 1998, *A&AS*, 127, 421
- Cayrel de Strobel, G., Soubiran, C., Friel, E. D., Ralit, N., & Francois, P. 1997, *A&AS*, 124,299
- Chavez, M., Stalio, R., & Holberg, J. B. 1995, *ApJ*, 449,280
- Collins II, G.W. & Sonneborn G.H. 1977, *ApJS*, 34, 41
- Cunha, K., & Lambert, D. L. 1992, *ApJ*, 399, 586
- Cunha, K., & Lambert, D. L. 1994, *ApJ*, 426, 170
- Davidson, A. 1990 in *Observatories in Earth Orbit and Beyond.*, ed. Y. Kondo (Dordrecht: Kluwer), 292
- Dixon, W. V. D., & Hurwitz, M. 1998, *ApJ*, 500, L29
- Edvardsson, B., Andersen, J., Gustafsson, B., Lambert, D. L., Nissen, P. E., & Tomkin, J. 1993, *A&A*, 275, 101
- ESA. 1997, *The Hipparcos and Tycho Catalogs*, ESA SP-1200
- Fitzpatrick, E.L. & Massa D. 1999, *ApJ*, 525, 1011
- Fracassini, M., Pasinetti-Fracassini, L.E., Pastori, L. & Pironi, R. 1988, *Bull. Inf. CDS* 35, 121

- Gómez, J. F., Trapero, J., Morales, C., & Orozco, V., Edelstein, J., Korpela, E., Lampton, M. 2000, Ap&SS, submitted
- González-Riestra, R. 1998, in Ultraviolet Astrophysics Beyond the IUE Final Archive, ESA-SP 413, ed. W. Wamsteker & R. González-Riestra, (Noordwijk: ESA), 707
- Gutiérrez-Moreno, A. & Moreno, H. 1968, ApJS, 15, 459
- He, L., Whittet, D.C.B., Kilkenny, D., Spencer Jones, J.H. 1995, ApJS, 101, 335
- Hauck, B. & Mermilliod, M. 1998, A&AS, 129,431
- Holberg, J. B., Forrester, W. T., Shemansky, D. E., & Barry, D. C. 1982, ApJ, 257, 656
- Hubeny, I., & Lanz, T. 1995, ApJ, 439, 875
- Hurwitz, M., & Bowyer, S. 1991, Adv. Space Res., 11, 217
- Kaiser, D. 1989, A&A, 222,187
- Kilambi, G. C., Nagar, P., & Kameswara Rao, N. 1992, ApJ, 13, 175
- Kurucz, R. L. 1993, ATLAS9 Stellar Atmosphere Programs and 2 kms grid, (Kurucz CD-ROM 19)
- Lejeune, Th., Cuisinier, F., & Buser, R. 1997, A&AS, 125, 229
- Leone, F., Manfré, M., & Catalano, F. A. 1995, A&A, 299, 520
- Longo, R., Stalio, R., Polidan, R.S., & Rossi, L. 1989, ApJ, 339, 474
- Luck, R. E., & Lambert, D. L. 1985, ApJ, 298, 782
- Llorente de Andrés, F., & Morales, C. 1979, A&A, 72, 318
- Llorente de Andrés, F., Muñoz, F., López Arroyo, M., & Morales, C. 1981, A&A, 98, 418
- Maeder, A. 1975, A&A, 42, 471
- Massa, D., & Fitzpatrick, E.L. 2000, ApJS, 126, 517
- Merrill, P. W., & Burwell, C. G. 1933, ApJ, 78, 87
- Molnar, M.R., Stephens, T.C., & Mallama, A.D. 1978, ApJ, 223,185
- Morales, C., Trapero, J., Gómez, J.F., Giménez, A., Orozco, V., Bowyer, S., Edelstein, J., Korpela, E., Lampton, M., & Cobb, J. 2000, ApJ, 530,403
- Nissen, P. E. 1988, A&A, 199, 146
- Pedersen, H. 1979, A&AS, 35, 313
- Penprase, B. E. 1992, ApJS, 83,273
- Porceddu, I., Benvenuti, P., & Krelowski, J. 1991, A&A, 248, 188

- Renson, P. Gerbaldi, F., & Catalano, F. A. 1991, *A&AS*, 89, 429
- Rogerson, J. B., Spitzer, L., Drake, J. F., Dressler, K., Jenkins, E. B., Morton, D. C., & York, D. G. 1973, *ApJ*, 181, L97
- Savage, B. D., Massa, D., Meade, M., & Wesselius, P. R. 1985, *ApJS*, 59, 397
- Snow, T.P., Allen, M.M., Polidan, R.S., 1990, *ApJ*, 359, L23
- Stalio, R., Sandel, B. R., Broadfoot, A. L., & Chavez, M. 1993, *Adv. Space Res.*, 13, 379
- Tumlinson, J., Shull, J.M., Rachford, B., Snow, T.P., Jenkins, E.B., Savage, B.D., Sembach, K.R., Sonneborn, G., York, D.G.; FUSE Science Team 1999, *AAS*, 195, 0608
- Walborn, N.R. 1976, *ApJ*, 205, 419
- Warren, W. H. 1976, *MNRAS*, 174, 111
- Zhang, E.-H. 1983, *AJ*, 88, 825

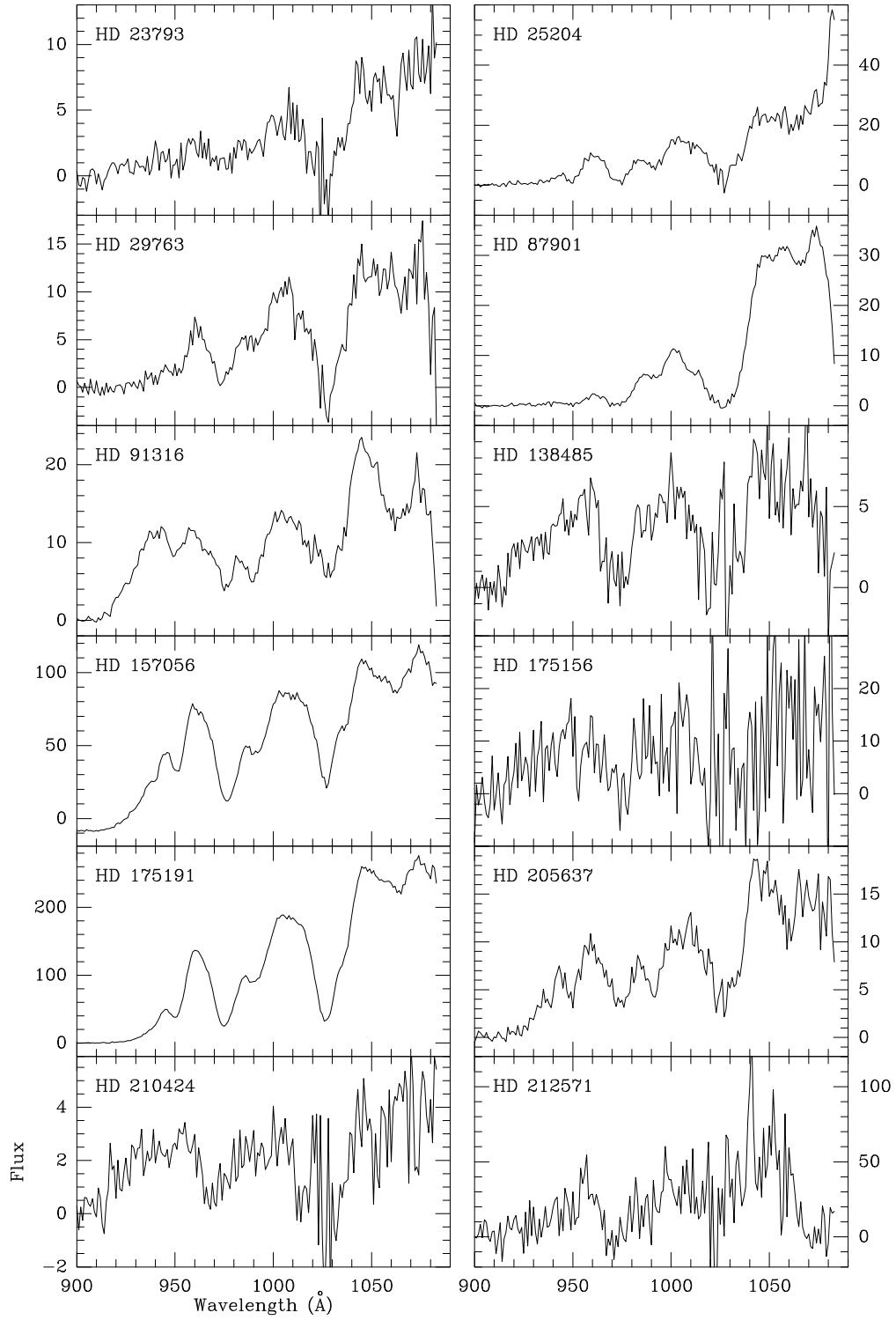


Fig. 1.— Spectra of the stars observed by EURD. The y axis represents the flux in units of $10^{-10} \text{ erg s}^{-1} \text{ cm}^{-2} \text{ \AA}^{-1}$.

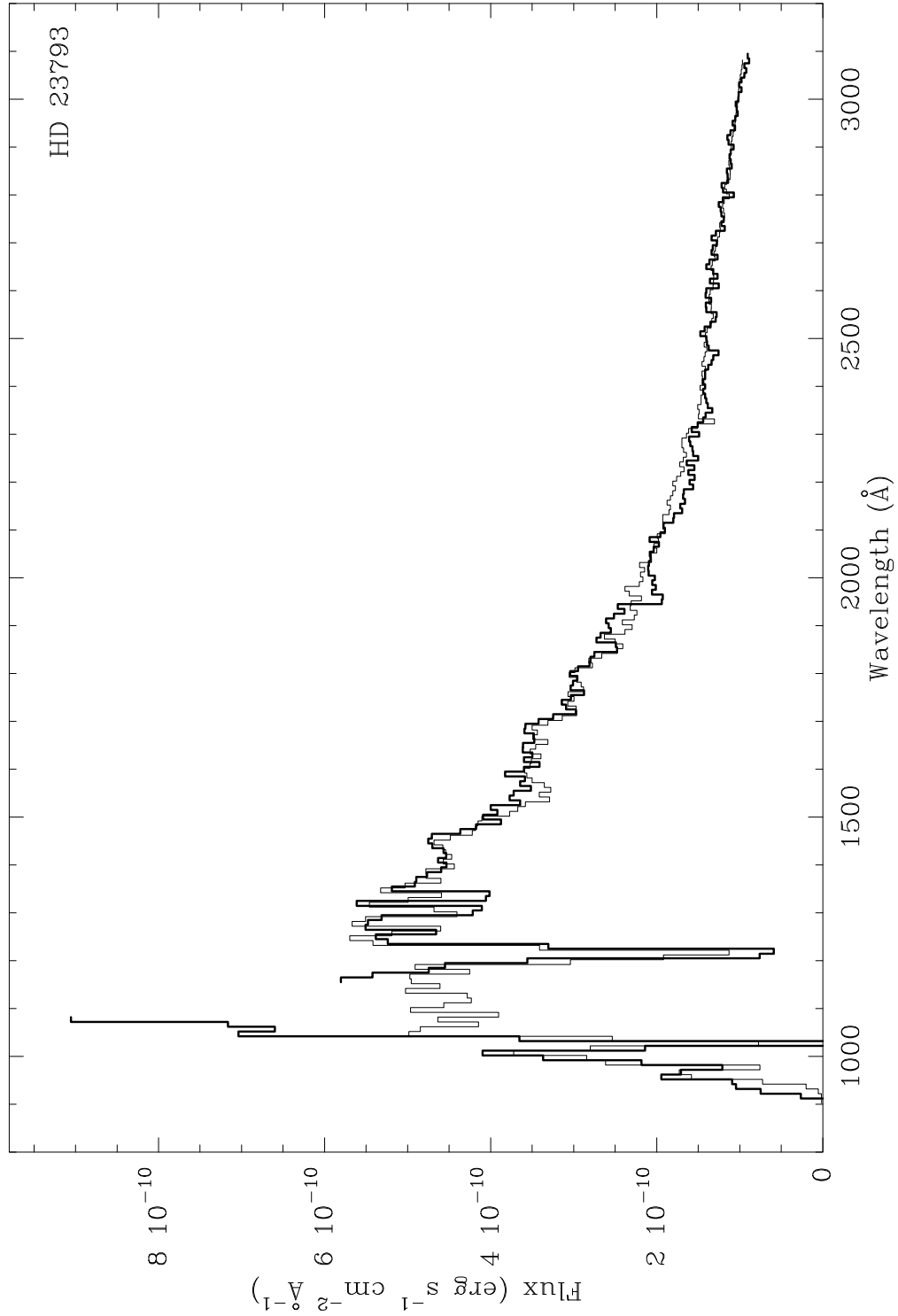


Fig. 2.— Spectra of HD 23793 as observed by EURD ($\lambda < 1070 \text{ \AA}$) and IUE ($\lambda > 1160 \text{ \AA}$) in heavy lines, superposed on the Kurucz model (thin line) that best fit the IUE data. Both EURD and IUE spectra have been binned down to match the spectral resolution of the model (10 \AA).

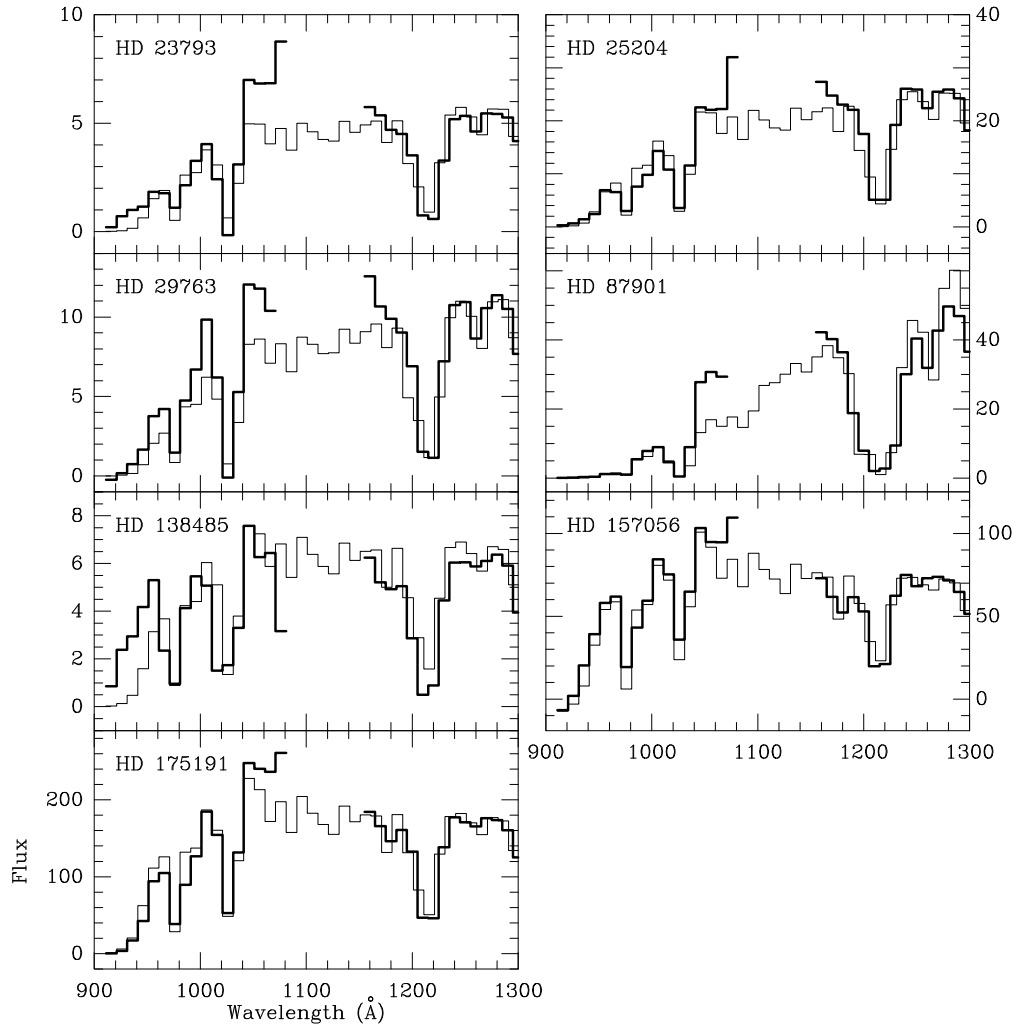


Fig. 3.— Spectra of main-sequence stars as observed by EURD (heavy line) and the model (thin line) that best fit the IUE data (heavy line, $\lambda > 1100 \text{ \AA}$). The y axis represents the flux in units of $10^{-10} \text{ erg s}^{-1} \text{ cm}^{-2} \text{ \AA}^{-1}$.

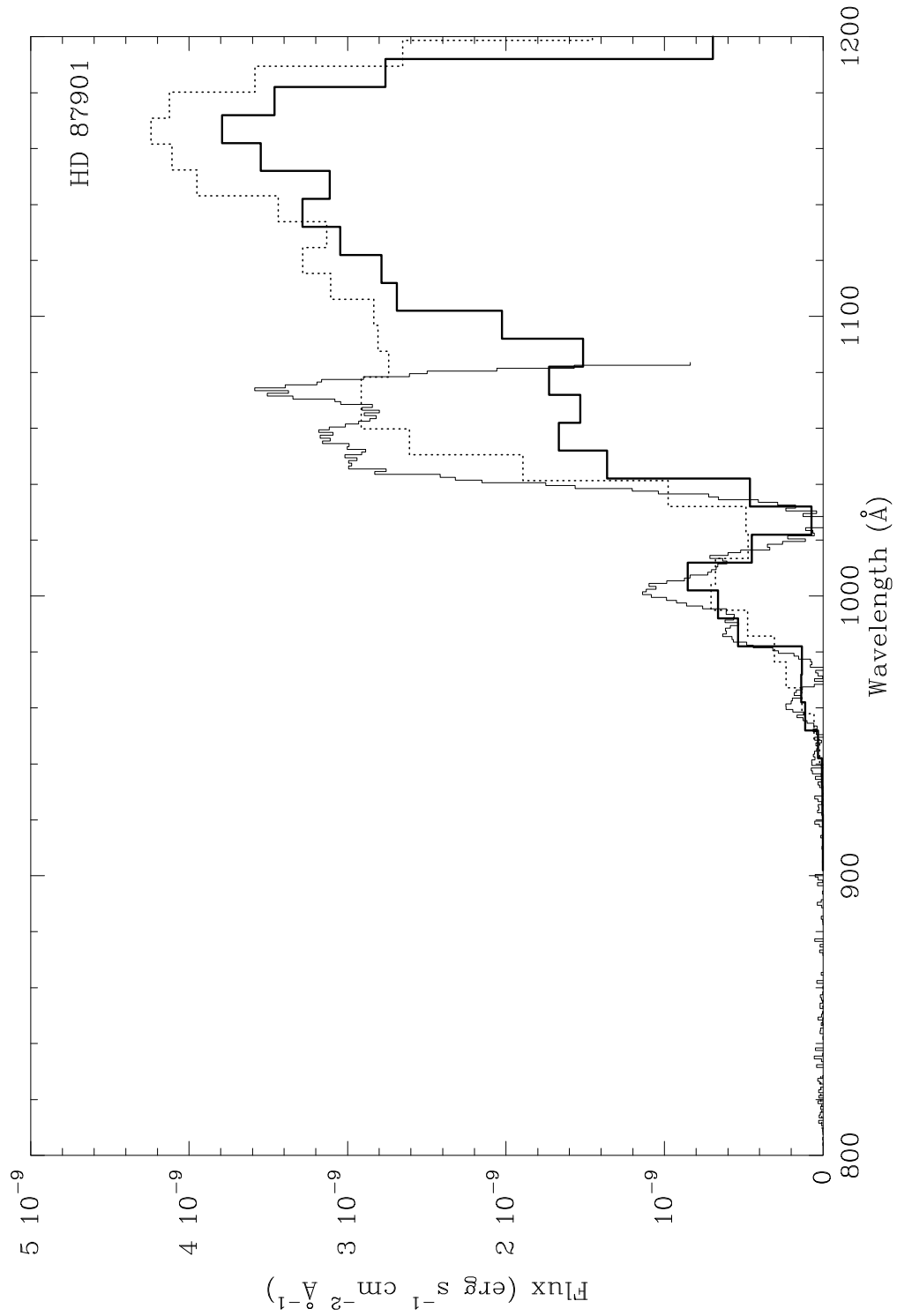


Fig. 4.— Spectra of HD 87901 (α Leo) as observed by EURD (thin line, $\lambda < 1070$ Å) (thin line) and Voyager (dotted line), superimposed on the Kurucz model (heavy line) that best fit the IUE spectrum.

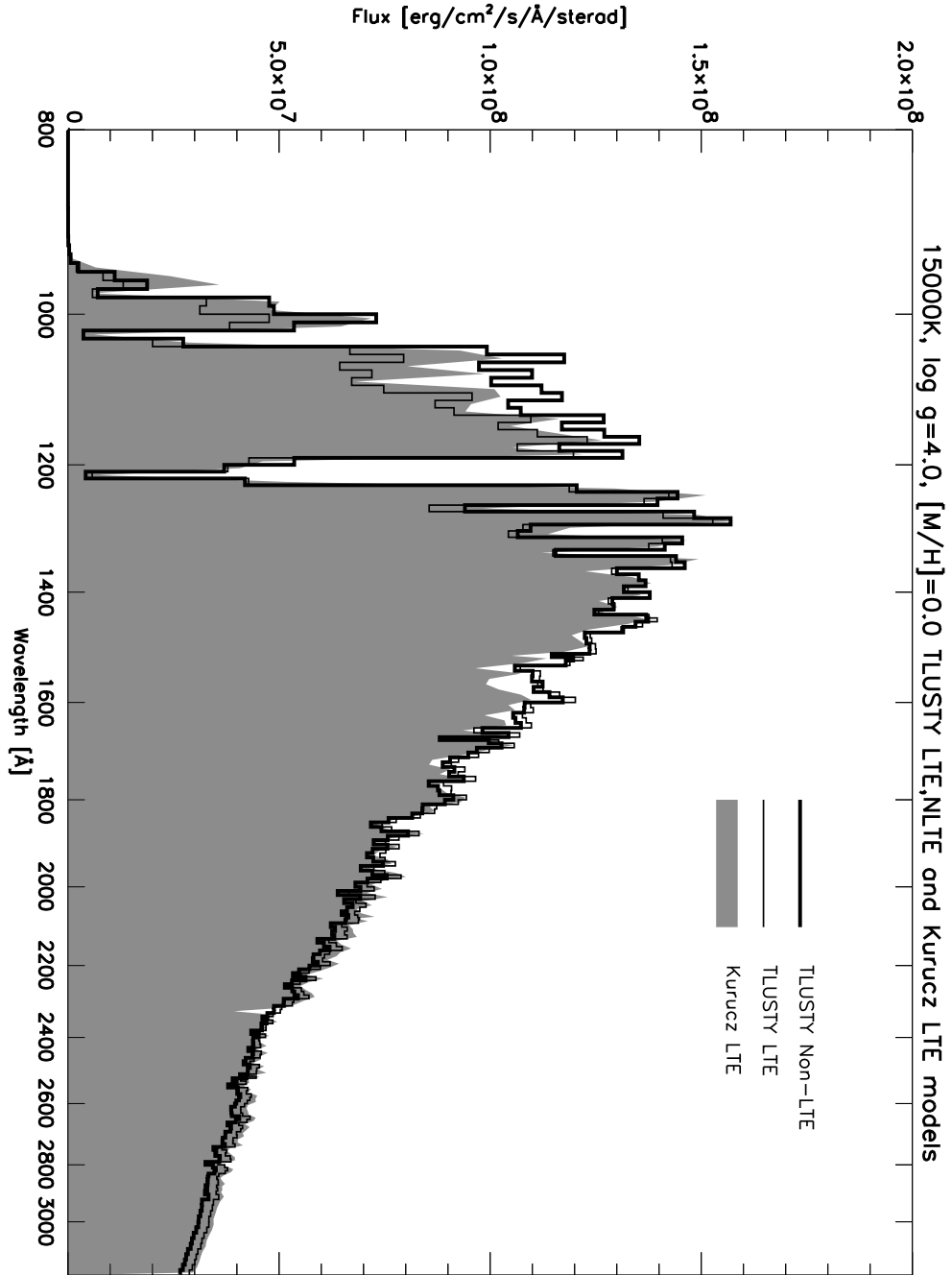


Fig. 5.— Comparison between synthetic spectra computed using TLUSTY LTE and non-LTE models for parameters $T_{eff} = 15000$, $\log g = 4.0$, $[M/H] = 0.0$. The corresponding Kurucz model flux is illustrated by the shaded region.

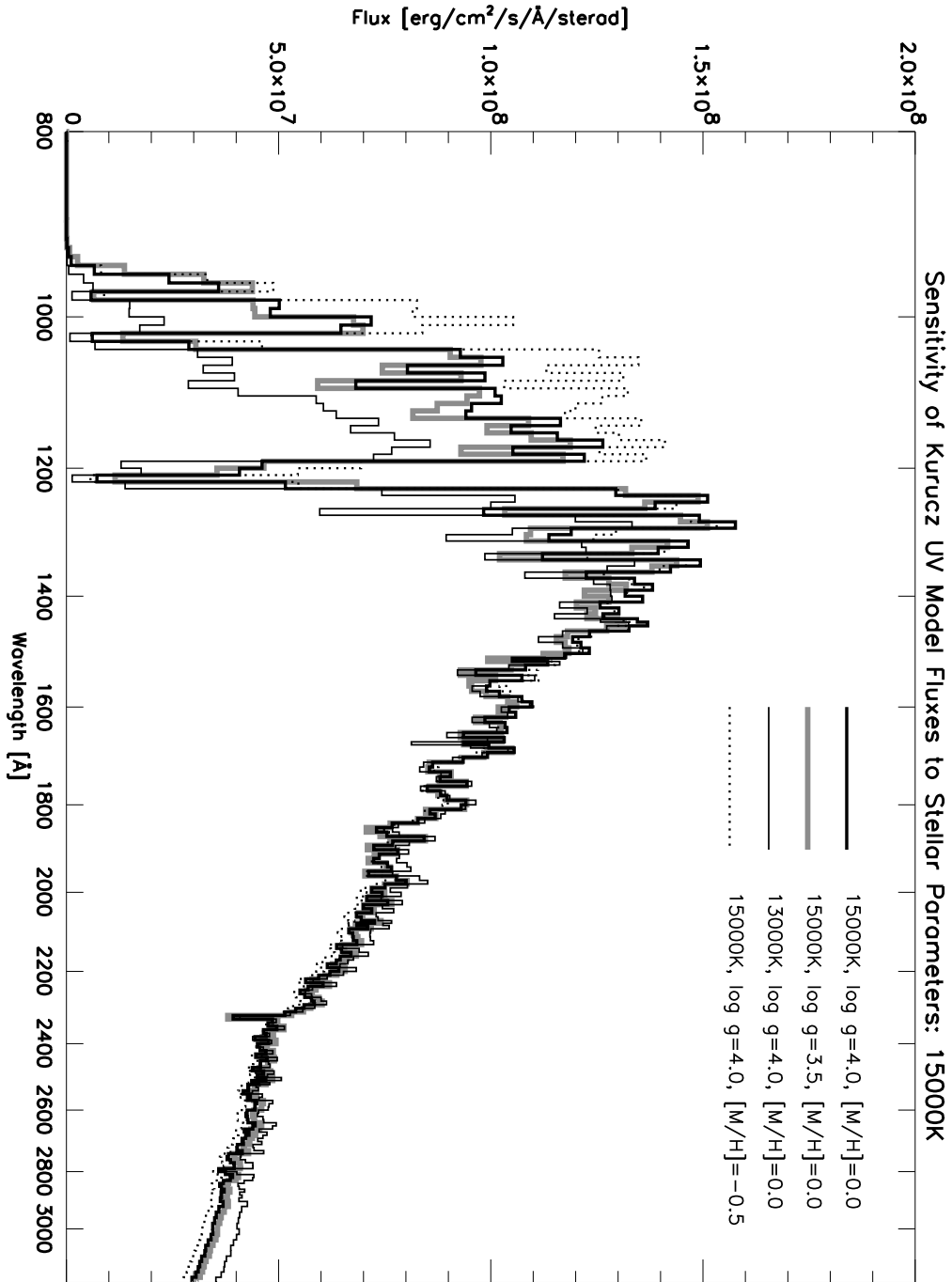


Fig. 6.— Comparison between Kurucz model UV and FUV fluxes to illustrate their sensitivities to stellar parameters. Illustrated are parameters 15000 K, $\log g = 4.0$, $[M/H] = 0.0$, and perturbations to this set orthogonally in temperature (-2000 K), surface gravity (-0.5) and metallicity (-0.5).

Table 1. Observation log

HD number	Year	Month	Days
HD 23793	1997	November	10–12
HD 25204	1997	November	11–13
HD 29763	1997	December	5–7
HD 87901	1998	February	18– 2
	1999	February	16, 19–20
HD 91316	1998	February	23–25
	1998	March	1–4, 6–8
	1999	February	27
	1999	March	7–8
HD 116658	1998	April	13–19
	1999	April	2–23
HD 138485	1998	May	11, 13–18
HD 157056	1998	June	13–17
HD 175156	1998	June	28–30
HD 175191	1998	July	3–7, 9, 11, 30
HD 205637	1997	August	14–17, 21–22
	1998	August	19
HD 210424	1998	August	23–27, 29
HD 212571	1997	August	23

Table 2. Observational parameters of the spectra

HD number	Total integration time (10^4 s)	noise level σ ^a (10^{-11} erg s ⁻¹ cm ⁻² Å ⁻¹)	signal to noise ^b
HD 23793	1.1150	6.2	7
HD 25204	2.1128	4.9	31
HD 29763	1.6725	4.9	20
HD 87901	7.3273	2.4	45
HD 91316	8.3627	2.9	44
HD 116658	10.9550	2.6	3662
HD 138485	1.7477	8.0	11
HD 157056	4.3473	3.7	219
HD 175156	0.3353	39.7	3
HD 175191	5.5884	3.2	514
HD 205637	4.6017	4.1	29
HD 210424	3.0884	5.1	8
HD 212571	0.4358	64.5	6

^aMeasured between 750 and 850 Å. Valid for wavelengths \lesssim 945 Å. For longer wavelengths, this noise level increases to a factor of 2 at \sim 1070 Å.

^bSignal measured at 1000 Å.

Table 3. Stellar parameters

HD number	Name	Spectral Type	V	E(B-V)	T_{eff} ^a (K)	EURD – Kurucz ^b $\lambda < 1010$	$\lambda > 1040$
Main Sequence Stars							
HD 23793	ϵ Tau	B3 V	5.06	0.0449	17800	0.24	0.57
HD 25204	λ Tau	B3 V	3.47	0.0582	18100	-0.11	0.21
HD 29763	τ Tau	B3 V	4.29	0.0389	16600	0.425	0.54
HD 87901	α Leo	B7 V	1.33	0.0382	13200	0.10	0.95
HD 138485	ζ Lib	B3 V	5.50	0.0453	19100	0.36	-0.15
HD 157056	θ Oph	B2 IV	3.26	0.0114	21700	0.08	0.13
HD 175191	σ Sgr	B2.5 V	2.078	0.00	19900	-0.13	0.22
Emission Line Stars							
HD 205637	ϵ Cap	B3 Vpe	4.70	0.0087	
HD 212571	π Aqr	B1 Ve	4.64	0.11	
Peculiar stars							
HD 91316	ρ Leo	B1 Ib	3.85	0.056	
HD 175156		B3 II	5.10	0.266	
HD 210424	ϵ Aqr	B5 III	5.42	0.0329	

^aFor peculiar and emission line stars no appropriate model could be fit.

^bRelative difference between EURD and Kurucz model for $\lambda < 1010 \text{ \AA}$ and $\lambda > 1040$ ([EURD – Kurucz]/Kurucz).

Table 4. IUE spectra from the INES archive

HD number	IUE Short Wavelength spectra	IUE Long Wavelength spectra
HD 23793	SWP20583RL.FITS	LWR16502RL.FITS
HD 25204	SWP18283HL.FITS	-
HD 29763	SWP45931HL.FITS	-
HD 87901	SWP33624LL.FITS	LWP08231LL.FITS
HD 116658	SWP33091HL.FITS	LWP13650HL.FITS
HD 138485	SWP35528LL.FITS	LWP15008LL.FITS
HD 157056	SWP04430RS.FITS	LWP24025RL.FITS
HD 175191	SWP16368RL.FITS	LWR12623RL.FITS